

Speeding-up MR acquisitions using ultrasound signals, and scanner-less real-time MR imaging

Frank Preiswerk¹, W. Scott Hoge¹, Matthew Toews¹, Jr-yuan George Chiou¹, Laurent Chauvin¹, Lawrence P. Panych¹, and Bruno Madore¹

¹Department of Radiology, Harvard Medical School, Brigham and Women's Hospital, Boston, MA, United States

Target Audience: Researchers and clinicians interested in real-time MRI and image-guided therapies.

Purpose: MRI and ultrasound (US) imaging have complementary properties and advantages, with great soft tissue contrast for the former and high acquisition rates for the latter. For this reason several noteworthy efforts have been made to combine the two imaging modalities¹⁻⁷. A characteristic of the approach pursued here is that the US transducer is very simple: The small 8mm-diameter single-element probe is held in place using an adhesive bandage (Fig. 1), and a flexible MR coil array can simply be wrapped over it. The emitted US field is not focused, it is expected to penetrate and reflect possibly several times within the abdomen, and the received signal acts as a unique signature of the internal organ arrangement at any given moment.

While there is nothing special about the US transducer itself, or the MR images being acquired, interesting behaviors emerge when detecting correlations between raw US signals and the MR images. After a training period extending roughly a few breathing cycles the US signal can become a surrogate for the MR imaging system. The US signal can be used to generate extra MR images in-between actually-acquired ones, to boost temporal resolution. Alternately, synthetic MR images can be generated even after the volunteer has been physically removed from the MR scanner, based solely on incoming US signals and previously-learned correlations between the two modalities. This intriguing ‘scanner-less real-time MRI’ behavior might, in principle at least, allow image-guided procedures to be performed outside the confines of the imaging bore.

Methods: Five volunteers were imaged with the hybrid US+MR setup, following informed consent. Fiber-optic probes monitored the temperature of the transducer and its cable, and scanning would have been stopped if either had exceeded body temperature (threshold at 38°C). The US transducer (Imasonic, 8mm, 5.8MHz) was held to the volunteer’s abdomen using an adhesive bandage, and a product 8-channel cardiac array was wrapped over it. The first 4 subjects were imaged using a single-slice acquisition (5mm-thick sagittal, 30° flip angle, FOV between 20 and 24cm, matrix size 128×96 or 128×128, TR between 7 and 15ms, MR temporal resolution between 0.48 and 1.15s, US frame rate = 1/TR, i.e., from 56 to 156Hz). The last subject was scanned instead with a 2-plane scheme (5mm slices, 30° flip angle, FOV=38cm, 192×192, TR=18ms, 75% partial-Fourier, two-fold parallel imaging, 0.58s per MR image, US frame rate = 56Hz).

For every incoming US trace $\mathbf{u} \in \mathbb{R}^p$, the n_1 -nearest (most similar) past traces were matched using Pearson’s correlation coefficient. The n_1 images associated with these n_1 traces were averaged, yielding a synthetic MR image for the present time point. The boost in temporal resolution provided by the algorithm was enormous, from about 20- to 100-fold in the datasets reconstructed here. Frame rates above 20-30Hz are beyond the abilities of human eyes, and so averaging was performed to bring frame rates down to ~25Hz. A sliding window was used to average n_2 previous estimations, see right term in Eq. 1, with $w_1 + w_2 = 1$.

The number of selected nearest matches, n_1 , is adjusted depending on their correlation score. The maximum number is $n_{1\max}$, and a smaller number gets used instead if there is a paucity of good matches. This situation may happen, for example, at the beginning of an exam when few time frames are available, or when rarely-seen motion such as especially-deep inspirations occur. In such cases when a small number of good matches are available, n_1 is kept small, and weight on the second term in Eq. 1, w_2 , is increased. This is formulated as a linear program $\text{argmax}_{n_1} \mathbf{c} = (c_1, \dots, c_{n_1})$ subject to the conditions $|\max(\mathbf{c}) - \min(\mathbf{c})| \leq w_\sigma \sigma_m$ and $n_1 \leq n_{1\max}$, where \mathbf{c} is the vector of correlation scores of the best n_1 matches, σ_m is the sliding-window standard deviation of the past m averages of \mathbf{c} and w_σ is a weight factor. Upon determination of n_1 , the weights in Eq. 1 are set to $w_1 = n_{1\max}/n_1$ and $w_2 = 1 - w_1$. The result is a flexible algorithm that adapts to the statistics of the ultrasound data stream: If the number of high-quality matches is low, the algorithm puts less trust in them and emphasizes the n_2 previous frames instead.

Results: The algorithm was applied to all acquired slices, including those of the sagittal-coronal scheme. As time progresses, the database of previously sampled data grows and with it the quality of synthetic MR images. Two 5s representative time segments are shown in Fig. 3 using an M-mode format. The superior-inferior motion of one image line through the liver gives rise to an oscillatory pattern in Fig. 3 during breathing. For the earlier segment on the left, note that motion appears much more natural and smooth for the 56Hz synthetic MR data than the 1.7Hz acquired MR data. For the later segment on the right, the MR stream of data had ended, yet synthetic MR images may still be generated based solely on the US signal. Parameters $n_{1\max} = 7, n_2 = 3 - 7, m = 100 - 400, w_\sigma = 3$ were employed here.

Discussion and Conclusion: Our algorithm produces an MR image stream with high temporal resolution after a learning phase of simultaneous MRI+US acquisitions, even after the subject is taken out of the scanner. While the results presented here were obtained offline, a real-time framework for MRI+US imaging and prediction is currently being developed, as shown in Fig. 4, based on 3D Slicer and OpenIGTLink⁸.

References: [1] Arvanitis CD et al. Phys Med Biol 2013;58(14):4749-61. [2] Petrusca L et al. Invest Radiol 2013;48(5):333-40. [3] Gunther M, Feinberg DA. MRM 2004;52(1):27-32. [4] Feinberg DA et al. MRM 2010;63(2):290-6. [5] Schwartz BM et al. MRM 2013;69(4):1023-33. [6] Toews M et al. ISMRM 2013:0478. [7] Kording F et al. ISMRM 2013:1421. [8] Slicer3d, <http://www.slicer.org>. Support from NIH grants P41EB015898, R01EB010195 and R01CA149342 is acknowledged.

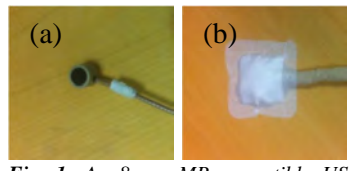


Fig. 1: An 8-mm MR-compatible US transducer (a) is placed in a holder along with fiber-optic temperature probes, and kept in place using an adhesive bandage (b).

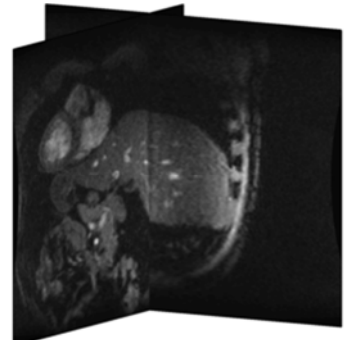


Fig. 2: Sagittal and coronal images are alternatingly acquired.

$$\tilde{I} = \frac{w_1}{n_1} \sum_k I_k + \frac{w_2}{n_2} \sum_h \tilde{I}_h \quad [1]$$

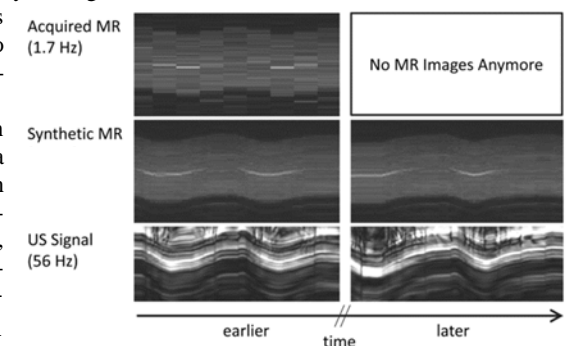


Fig. 3: M-mode visualization of the sagittal slice from our two-slice (sagittal and coronal) dataset.

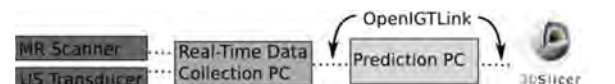


Fig. 4: Overview of the real-time system being developed, whereby both streams of information are sampled, processed and fed into 3D Slicer for display.